Metal atomic contacts under defined environmental conditions

Tomoka Nakazumi[1], Daigo Murai[1], Kazuhito Tsukagoshi[2], Manabu Kiguchi[1*]

1 Department of Chemistry, Graduate School of Science and Engineering, Tokyo Institute of Technology, 2-12-1 W4-10
Ookayama, Meguro-ku, Tokyo 152-8551, Japan
2 WPI Center for Materials Nanoarchitechtonics (WPI-MANA), National
Institute for Materials Science, Tsukuba, Ibaraki 305-0044, Japan
* Corresponding author: e-mail: kiguti@chem.titech.ac.jp

We have developed a measurement system for investigating metal atomic contacts under defined environmental conditions (0.1 Pa–10^5 Pa, 4 K–300 K). Using this newly developed system, the conductance behavior and lifetime of Au atomic contacts were investigated in vacuum and in an oxygen atmosphere (~10^5 Pa) at room temperature. The conductance curves and conductance histograms of the Au contacts in vacuum agreed with those measured in the oxygen atmosphere, indicating a weak interaction between oxygen and Au atomic contact. While the conductance behavior was not affected by the presence of oxygen, the lifetime of the Au atomic contact was slightly increased by the presence of oxygen.
Key words: metal atomic contact, quantized conductance, mechanically controllable break junction, self-breaking

1. INTRODUCTION

The investigation of electron transport through metal atomic contacts is of great interest in both fundamental quantum physics and nanotechnology [1]. Recent developments in experimental techniques including scanning tunneling microscope (STM) break junctions and mechanically controllable break junctions (MCBJ) enable us to fabricate and investigate metal atomic contacts in various conditions, such as ultra high vacuum (UHV), ambient conditions including electrochemical environments [2-8]. Detailed investigations have been carried out in UHV at low temperatures (~4 K), because clean and stable metal atomic contacts can be fabricated under these conditions, and spectroscopic techniques including inelastic tunneling electron spectroscopy and point contact spectroscopy can be utilized at low temperatures [2-5]. Conductance quantization, electron-phonon interaction, Kondo effects, and other interesting phenomena have also been observed for metal atomic contacts under UHV at low temperatures [1,3,5].

The interaction between metal atomic contacts and molecules is one of the current topics in the research field of metal atomic contacts. The conductance of Au and Cu atomic contacts decreases from 1 G_0 ($2e^2/h$) to 0.5 G_0 by introducing CO to the contact at 4 K, which was explained by the scattering of the conduction electrons by the CO molecules adsorbed on the metal atomic contacts [9]. The adsorption of hydrogen molecules on Co or Pd atomic contacts decreases the conductance of the metal atomic contacts, together with the stabilization of the metal atomic contact [10,11]. The stabilization of the Co and Pd contacts leads to the formation of the single atomic chains. Here, it is noteworthy that atomic chains are not formed for clean Co and Pd contacts. In some metals, single molecular junctions can be formed by introducing molecules to the

metal atomic contacts. Single hydrogen molecular junctions are fabricated by breaking the Pt atomic contacts in a hydrogen atmosphere [12,13]. The formation of a single hydrogen molecular junction was reported for Au and Cu atomic contacts [14-17].

The interaction between metal atomic contacts and molecules has been investigated at low temperatures in detail, using conductance, vibration spectroscopy, shot noise, and other techniques. The next subject of interest is the temperature dependence of the interaction between metal atomic contacts and molecules, especially at room temperatures, for the following reasons. First, the interaction between molecules and the metal substrate can vary with the temperature. For example, an ethylene molecule adsorbs on Pt(111) via π-bonding at temperatures below 52 K; above this temperature, the ethylene molecule changes its conformation to a di-σ-bonded species [18]. The adsorption structure of molecules on metal contacts could vary with the temperature, as with the case on a metal substrate. Second, the phase of the molecule changes with the temperature. At low temperature (~4 K), molecules are in a liquid or solid phase. The previous studies carried out at low temperature investigated the interaction between condensed phase molecules and the metal atomic contacts. The interaction between the metal atomic contacts with molecules in the gas phase can be different from that in the condensed phase. Investigation into molecules in the gas phase and metal atomic contacts at room temperature is an important subject, especially for applications as a gas sensor. Despite the potential interest in the interaction between the metal atomic contacts and molecules at room temperature, there are few studies that exist. We have thus developed a measurement system in order to investigate the metal atomic contacts under defined environmental conditions.

In this study, the conductance behavior of Au atomic contacts was investigated in vacuum and in an oxygen atmosphere.

2. MEASUREMENT SYSTEM

The metal atomic contacts are fabricated using the MCBJ technique [1,19]. Fig. 1(a) shows a schematic view of the MCBJ setup. A metal wire is fixed on the bending beam as substrate. The substrate is mounted in a three-point bending configuration between the top of a stacked piezo element and two fixed counter supports. The substrate is bent by moving the piezo element forward. The bending causes the top surface of the substrate to expand. At some critical strain, the wire finally breaks, forming two separate electrodes. By relaxing the bending of the substrate, the contact is re-established. By controlling the bending of the substrate with the piezo element, the relative displacement of the two electrodes can be precisely controlled, which enables us to fabricate the metal atomic contact.
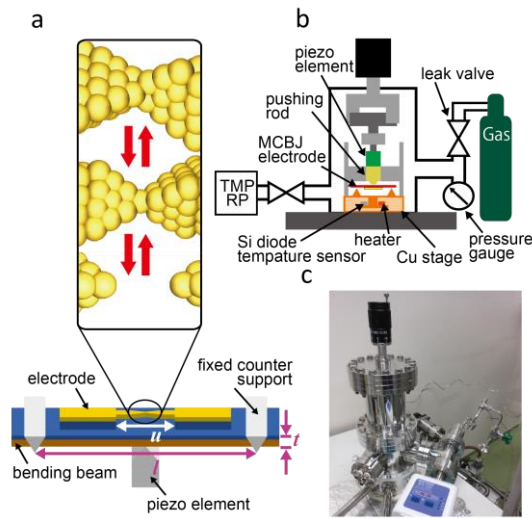

Fig. 1: (a) Schematic view of the MCBJ setup. (b) Schematic side view of the measurement system for metal atomic contacts under defined environmental conditions. (c) Photo image of the measurement system.

Fig. 1(b, c) show the schematic side view and digital photo of the measurement system for metal atomic contacts under defined environmental conditions. The MCBJ setup is fixed on the Cu stage, which can be cooled down to 4.2 K in vacuum by flowing liquid He into the tube connected to the Cu stage. The temperature of the Cu stage is measured with the diode temperature monitor (see Fig. 1(b)). The resistance heater is attached to the Cu stage. The temperature of the Cu stage (4 K~300 K) can be freely controlled by tuning the heater power and liquid He flow rate. While the MCBJ sample is directly contacted with the Cu stage, the pushing rod is thermally disconnected with the support

whose temperature is 300 K. Therefore, we can assume that the temperature of the contact is the same as that of the Cu stage. The temperature fluctuation of the Cu stage can be less than 3 K by controlling the heater power. We can obtain the thermal stability to allow measurements within 10 minutes in this setup. The vacuum chamber is evacuated by a turbo molecular pump (TMP). To introduce molecules to the metal contacts, a gas doser is mounted on the vacuum chamber. The amount of gas introduced to the metal contact is monitored with the pressure gauge. The pressure in the chamber (0.1 Pa~10^5 Pa) is controlled by tuning the gas flow rate using a leak valve and pumping speed using a valve. The pressure fluctuation is less than 10 % in this setup.

The Au MCBJ sample is fabricated using a lithographic technique [20-22]. A polished phosphor bronze substrate (length 25 mm, width 4 mm, thickness 0.5 mm) is spin-coated (500 rpm for 5 s and 3000 rpm for 60 s) with a polyimide layer for electrical insulation. The thickness of the polyimide layer is about 5 μm. Nanoscale Au junctions (narrowest constriction ~150 nm × 150 nm) are fabricated on the polyimide-coated substrate using electron beam lithography and a lift-off technique. Metal (Au/Ti, 150 nm/3 nm) is deposited by thermal deposition. Subsequently, the polyimide underneath the Au junctions is removed by oxygen plasma etching (O_2 80 sccm 80 W), and a freestanding Au nanobridge of length, u (~4 μm), is obtained. Figure 2 shows a schematic view and a scanning electron microscopy image of the nano-fabricated Au MCBJ sample. As a result of the chosen geometry, the MCBJ setup itself acts as a reduction gear for the motion of the piezo element (δx) with respect to the relative displacement of the two electrodes (δy). For the ideal case of homogeneous strain in the bending beam, the displacement ratio (r) between δy and δx is given by $r = \delta y/\delta x = 6tu/l^2$, where t, u, and l are thickness of the bending beam [see Fig. 1(a)], the distance between the fixed parts of the electrode, and the distance between the two counter supports, respectively [20-22]. The displacement ratio is 2×10^{-5} for the present setup, with $l = 20$ mm, $t = 0.5$ mm, and $u = 4$ μm. The piezo element (APA150M) has a displacement of 1.1 μm V^{-1}. Considering the displacement ratio of 2×10^{-5} in this setup, δy is estimated to be 22 pm when 1 V is applied to the piezo element. DC two-point voltage-biased conductance is measured with Keithley 428. A personal computer controls the movement of the piezo element via a high voltage source and a standard data-acquisition board (National Instruments) is installed in the personal computer.
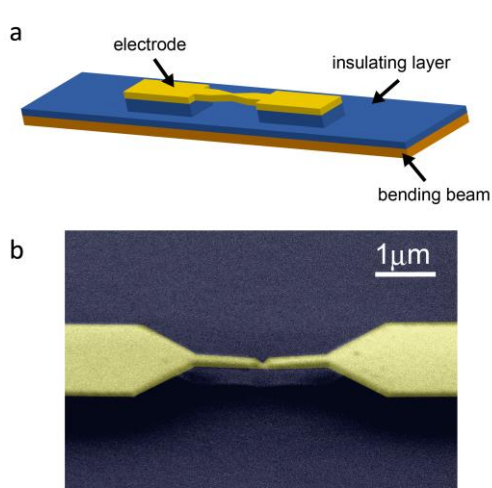
Fig. 2: (a) Schematic view and (b) SEM image of the nano-fabricated Au MCBJ sample.

3. CONDUCTANCE MEASUREMENT

Fig. 3(a) shows examples of the conductance curves during stretching of Au contacts in air. The conductance decreased in a stepwise fashion, by integer multiples of G_0. The corresponding conductance histogram [Fig. 3(b)] showed well defined peaks at near-integer multiples of G_0. When the cross-section of a metal contact is reduced to a few atoms, the Fermi wavelength of the electrons becomes comparable to the contact diameter, and quantum-mechanical effects govern the electron transport properties. As a consequence, conductance of the metal nanocontacts is expressed by $G = (2e^2/h)\Sigma T_i$ where T_i is the transmission probability of the i-th conductance channel, e is the electron charge, and h is Planck's constant [1]. $G_0 = 2e^2/h$ is the unit of the quantized conductance. The transmission probability depends on the chemical valence of the metal and on the atomic configuration of the contact. In the case of contacts of group 11 metals, the conduction channel is a single s channel with a transmission probability of 1. Therefore, the conductance is quantized in units of G_0 for the Au contacts, and the conductance of the Au atomic contact is 1 G_0. The appearance of the clear 1 G_0 steps in the conductance curves and 1 G_0 peaks in the conductance histograms indicated that we successfully fabricated the Au atomic contact using our newly developed measurement system.
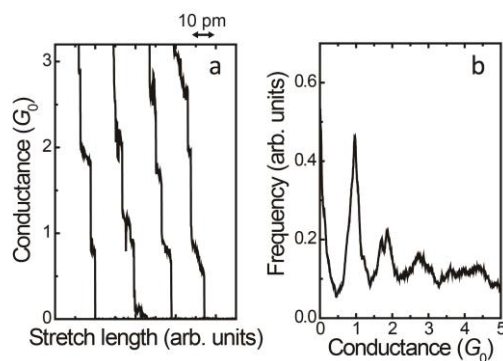

Fig. 3: (a) Examples of conductance curves during the stretching of Au contacts in air. The bias voltage was 0.05 V. (b) Conductance histogram constructed from 1000 conductance curves.

We then investigated the Au atomic contacts under the defined environmental conditions. Figure 4 shows the conductance curves and conductance histograms of the Au contacts measured in vacuum (0.1 Pa) and in an oxygen atmosphere (2×10^5 Pa) at room temperature. Clear 1 G_0 steps and 1 G_0 peaks were observed in the conductance curves and histograms. The conductance behavior of the Au contacts was close to that of the Au contacts measured in air. Au is an inert metal, and thus the interaction between the molecules and the Au atomic contact would be small. Therefore, the conductance behavior of the Au atomic contact was not affected by the presence of oxygen, air at room temperature. A previously reported study at 4 K showed that the conductance behavior of Au atomic contacts was not affected by the introduction of oxygen, similar to the present study measured at room temperature [23].

We then investigated the lifetime of the Au atomic contacts under the defined environmental conditions. The lifetime of the Au atomic contact was evaluated from the conductance curves during self-breaking of the Au contacts [Fig. 5(a)], under the following process. The self breaking is a thermally activated fracture of the Au atomic contact at room temperature. First, the Au nanocontacts were stretched until the conductance of the nanocontact was around 2 G_0. We then fixed the electrode separation, and measured the conductance of the Au nanocontacts during the self-breaking process. Finally, the lifetime of the Au atomic contact was obtained as the period that the contact conductance remained at 1 G_0. Since the conductance of the Au atomic contact fluctuated with time and contact because of thermal fluctuations and variations in the conformation of the atomic contact, we defined the single atomic contact as the region where the conductance of the contact was between 1.3 G_0 and 0.7 G_0. Figure 5(b) shows the distribution of the lifetime of the Au atomic contacts in vacuum (0.1 Pa) at room temperature. The average lifetime of the Au atomic contact was determined to be 5 s by fitting the experimental data with a Gaussian function.
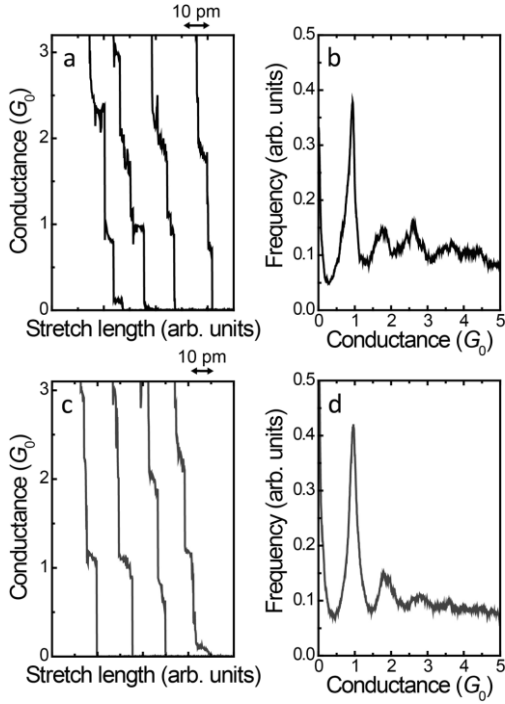
Fig. 4: Examples of conductance curves during the stretching of Au contacts in (a) vacuum (0.1 Pa) and (c) oxygen atmosphere (2×10^5 Pa) at room temperature. The bias voltage was 0.05 V. The conductance histograms of Au contacts in (b) vacuum and (d) oxygen atmosphere. The conductance histograms were constructed from 1000 conductance curves.

Since the Au atomic contact undergoes a thermally activated fracture at room temperature, the lifetime of the Au atomic contact is described in Arrhenius form as

$$\tau = \frac{1}{f} \times \exp\left(\frac{E_B - \alpha V - \beta F}{k_B T_{eff}}\right)$$

$$T_{eff}^4 = T_0^4 + T_V^4 \qquad (1)$$

where f, E_B, T_{eff}, and T_0 are the Einstein frequency, energy barrier for breaking the contact, effective contact temperature, and ambient temperature, respectively [25]. The Einstein frequency has been calculated analytically as 7×10^{12} Hz for Au atomic chains in a previously reported study [26]. The effective energy barrier decreases as a function of the external tensile forces, αF, and the current induced forces, ζV. Local ionic heating contributes to contact destabilization through $T_V = \Gamma (LV)^{1/2}$, where L and Γ are the effective chain length and a material dependent parameter, respectively. The lifetime exponentially depends on E_B, which depends on the atomic configuration of the contacts. Since it is not possible to control the atomic configuration of the contact and reproduce an identical atomic configuration, E_B varied from contact to contact, leading to the wide spread in lifetimes of the Au atomic contacts as shown in Fig. 5(b). Using the parameters $\alpha = 0.14$ eV/nN [26], $F = 0$ nN, $\Gamma = 60$ KV$^{-1/2}$ nm$^{-1/2}$ [26], $L \approx 1$ nm, $V = 0.05$ V, and $T_0 = 295$ K, E_B was calculated to be 0.79 eV, which agreed with the previously reported

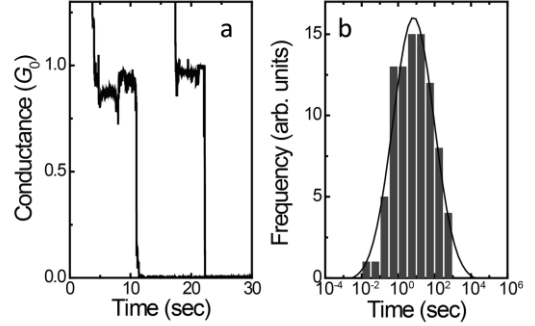theoretical calculation results [26].

Fig. 5: (a) Conductance curves during self-breaking of Au atomic contacts in vacuum (0.1 Pa) at room temperature. The bias voltage was 0.05 V. (b) Distribution of lifetime of Au atomic contacts obtained from 87 conductance curves in vacuum.

Finally, we show the preliminary results of the lifetime of the Au atomic contacts under the oxygen atmosphere (2×10^5 Pa) at room temperature using our newly developed system. Figure 6(a) shows the typical conductance curves during the self-breaking of the Au contacts in the oxygen atmosphere. The length of the 1 G_0 plateau seems to increase compared to that measured in vacuum. Figure 6(b) shows the distribution of the Au atomic contact lifetimes in the oxygen atmosphere. The average lifetime was 20 s, and E_B was calculated to be 0.82 eV, using Equation (1). The present results suggested that the lifetime of the Au atomic contacts was enhanced in the oxygen atmosphere. The stabilization of the Au atomic contacts can be explained by the decrease in surface energy, increase in the effective coordination number of the Au atomic contact induced by the adsorption of oxygen on the Au atomic contact, effective heat dissipation in the Au atomic contact, and by other reasons [27]. Further investigation into bias voltage dependence and pressure dependence would confirm the increase in the stability, and the stabilization mechanism.

4. CONCLUSIONS

We have developed a new measurement system in order to study the conductance behavior of metal atomic contacts under defined environmental conditions. Using this newly developed system, the Au atomic contacts were successfully fabricated in vacuum and in an oxygen atmosphere at room temperature. The conductance behavior and lifetime were investigated for the fabricated Au atomic contact. While the conductance behavior was not affected by the presence of oxygen ($\sim10^5$ Pa), the lifetime of the Au atomic contact was slightly increased. We also evaluated the energy barrier for breaking the Au atomic contacts based on a thermal activation model. The energy barrier was evaluated to be 0.79 eV for the Au atomic contacts in vacuum.
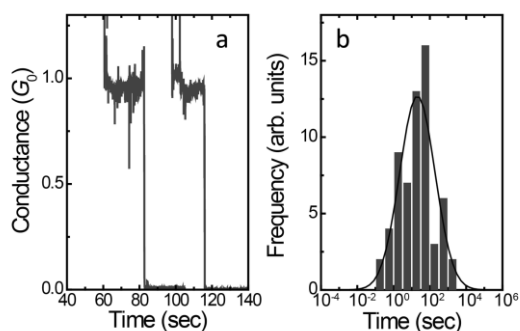
Fig. 6: (a) Conductance curves during self-breaking of Au atom-sized contacts in oxygen atmosphere (2×10^5 Pa). The bias voltage was 0.05 V. (b) Distribution of lifetime of Au atom contacts obtained from 62 conductance curves in oxygen atmosphere.

References

[1] N. Agraït, A. L. Yeyati, and J. M. van Ruitenbeek, *Phys. Rep.*, **377**, 81-279 (2003).

[2] A. Yanson, G. Bollinger, H. Van den Brom, N. Agraït, and J. M. van Ruitenbeek, *Nature*, **395**, 783-785 (1998).

[3] R. Smit, C. Untiedt, A. Yanson, and J. Van Ruitenbeek, *Phys. Rev. Lett.*, **87**, 266102/1-266102/4 (2001).

[4] N. Agraït, C. Untiedt, G. Rubio-Bollinger, and S. Vieira, *Phys. Rev. Lett.*, **88**, 216803/1-216803/4 (2002).

[5] M. R. Calvo, J. Fernández-Rossier, J. J. Palacios, D. Jacob, D. Natelson, and C. Untiedt, *Nature*, **458**, 1150-1153 (2009).

[6] J. Tian, Y. Yang, X. Zhou, B. Schcllhorn, E. Maisonhaute, Z. Chen, F. Yang, Y. Chen, C. Amatore, B. Mao, and Z. Tian, *ChemPhysChem*, 11, 2745 – 2755 (2010).

[7] Y. Yang, J. Liu, Z. Chen, J. Tian, Xi Jin, B. Liu, X. Li, Z. Luo, M. Lu, F. Yang, N. Tao and Z. Tian, *Nanotechnology* **22,** 275313 (2011).

[8] L. Grüter, M. T. González, R. Huber, M. Calame, and C. Schönenberger, *Small* **1**, 1067-1070 (2005).

[9] M. Kiguchi, D. Djukic, and J. M. van Ruitenbeek, *Nanotechnology*, **18**, 035205/1-035205/5 (2007).

[10] M. Kiguchi, K. Hashimoto, Y. Ono, T. Taketsugu, and K. Murakoshi, *Phys. Rev. B*, **81**, 195401/1-195401/5 (2010).

[11] T. Nakazumi and M. Kiguchi, *J. Phys. Chem. Lett.*, **1**, 923-926 (2010).

[12] R. H. M. Smit, Y. Noat, C. Untiedt, N. D. Lang, M. C. van Hemert, and J. M. van Ruitenbeek, *Nature*, **419**, 906-909 (2002).

[13] M. Kiguchi, R. Stadler, I. Kristensen, D. Djukic, and J. M. van Ruitenbeek, *Phys. Rev. Lett.*, **98**, 146802/1-146802/4 (2007).

[14] S. Csonka, A. Halbritter, G. Mihály, E. Jurdik, O. Shklyarevskii, S. Speller, and H. van Kempen, *Phys. Rev. Lett.*, **90**, 116803/1-116803/4 (2003).

[15] S. Csonka, A. Halbritter, and G. Mihály, *Phys. Rev. B*, **73**, 075405/1-075405/6 (2006).

[16] M. Kiguchi, T. Nakazumi, K. Hashimoto, and K. Murakoshi, *Phys. Rev. B*, **81**, 045420/1 (2010).

[17] R. Matsushita, S. Kaneko, T. Nakazumi, and M. Kiguchi, *Phys. Rev. B*, **84**, 245412/1-245412/5 (2011).

[18] J. M. Essen, J. Haubrich, C. Becker, and K. Wandelt, *Surf. Sci.*, **601**, 3472-3480 (2007).

[19] T. Nakazumi, S. Kaneko, R. Matsushita, and M. Kiguchi, *J. Phys. Chem. C*, **116**, 18250-18255 (2012).

[20] T. Nakazumi, Y. Wada, and M. Kiguchi, *Nanotechnology*, **23**, 405702/1-405702/6 (2012).

[21] K. Yokota, M. Taniguchi, M. Tsutsui, and T. Kawai, *J. Am. Chem. Soc.*, **132**, 17364-17365 (2010).

[22] J. M. van Ruitenbeek, A. Alvarez, I. Piñeyro, C. Grahmann, P. Joyez, M. H. Devoret, D. Esteve, and C. Urbina, *Rev. Sci. Instrum.*, **67**, 108 (1996).

[23] J. L. Costa-Krämer, *Phys. Rev. B*, **55**, R4875-R4878 (1997).

[24] W. Thijssen, D. Marjenburgh, R. Bremmer, and J. van Ruitenbeek, *Phys. Rev. Lett.*, **96**, 026806/1-026806/4 (2006).

[25] M. Tsutsui, K. Shoji, M. Taniguchi, and T. Kawai, *Nano Lett.*, **8**, 345-349 (2008).

[26] T. Todorov, J. Hoekstra, and A. Sutton, *Phys. Rev. Lett.*, **86**, 3606-3609 (2001).

[27] H.X. He, C. Shu, C.Z. Li, N.J. Tao, *J. Electroanal. Chem.* **522**, 26-32 (2002).